*Graphical Abstract

Graphical Contents List

Gelatin-pectin composite films from polyion complex hydrogels

Stefano Farris[1,*], Karen M. Schaich[2], LinShu Liu[3], Peter H. Cooke[3], Luciano Piergiovanni[1], Kit L. Yam[2]

[1]Department of Food Science and Microbiology – Packaging laboratory
University of Milan Via Celoria, 2 - 20133 Milan, Italy

[2]Department of Food Science, Rutgers University, 65 Dudley Road,
New Brunswick, New Jersey 08901, USA

[3]Eastern Regional Research Center, United States Department of
Agriculture, 600 East Mermaid Lane, Wyndmoor, Pennsylvania
19038, USA

*Corresponding Author. Tel: +390250316654; fax: +39 0250316672
E-mail address: stefano.farris@unimi.it (S. Farris)

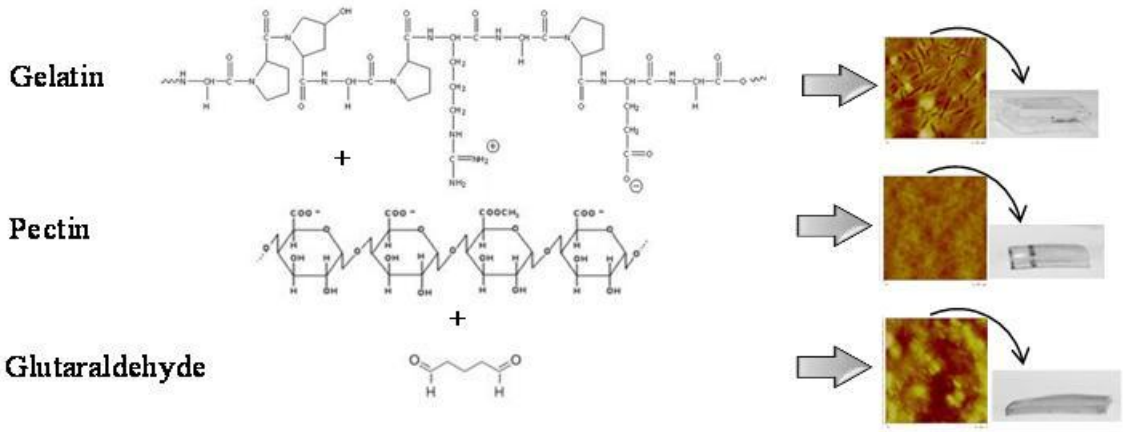

Gelatin-pectin composite films from polyion complex hydrogels

Stefano Farris[1,*], Karen M. Schaich[2], LinShu Liu[3], Peter H. Cooke[3], Luciano Piergiovanni[1], Kit L. Yam[2]

[1]Department of Food Science and Microbiology – Packaging laboratory
University of Milan Via Celoria, 2 - 20133 Milan, Italy

[2]Department of Food Science, Rutgers University, 65 Dudley Road,
New Brunswick, New Jersey 08901, USA

[3]Eastern Regional Research Center, United States Department of
Agriculture, 600 East Mermaid Lane, Wyndmoor, Pennsylvania
19038, USA

*Corresponding Author. Tel: +390250316654; fax: +39 0250316672
E-mail address: stefano.farris@unimi.it (S. Farris)

ABSTRACT

Preparation and properties of composite films from gelatin and low-methoxyl pectin from simultaneous reversible and permanent polyion complex hydrogels are presented. Ionic interactions between positively charged gelatin and negatively charged pectin produce reversible physical hydrogels with homogeneous molecular arrangement that improve both mechanical and water resistance but do not alter thermal stability relative to single polymer gels. Subsequent addition of 0.3 weight percent (wt.-%) glutaraldehyde crosslinks gelatin heterogeneously, due to the presence of domains with non-uniform crosslinking, as revealed by the structural analysis. Resulting interspersed permanent chemical hydrogel showed a decreased swelling attitude by nearly 10 fold relative to films from gelatin alone and further improved mechanical performance (tensile strength and elongation at break). Results demonstrate that simultaneously exploiting the specific reactivity provided by the functional groups of both biopolymers can be used to create unique new structures with improved properties and offer potential for tailoring these to a wide range of targeted applications.

Keywords: AFM; crosslinking; electrostatic interactions; hydrogel films; SEM

1. Introduction

The past few years have witnessed rapidly expanding interest in renewable agricultural feedstocks and marine food processing wastes as sources of biomolecules with potential to replace synthetic polymers (Tharanathan, 2003) in fabricating biomaterials with bioactivity, biocompatibility, biodegradability, and novel properties for unique applications (Lin & Metters, 2006). As biomolecules have become more available, ever-increasing demand for high-performance "natural" matrices for biomedical and pharmaceutical applications such as tissue engineering (Khademhosseini & Langer, 2007) and organ regeneration (Skotak, Leonov, Larsen, Noriega, & Subramanian, 2008; Jaklenec, Wan, Murray, & Mathiowitz, 2008; Lai, Lu, Chen, Tabata, & Hsiue, 2006), controlled drug delivery systems (Ghaffari, Navaee, Oskoui, Bayati, & Rafiee-Tehrani, 2007; Wei, Sun, Wu, Yin, & Wu, 2006; Kurisawa & Yui, 1998), bioadhesives for wound dressing (Ong, Wu, Moochhala, Tan, & Lu, 2008), films, contact lenses, and capsules for oral ingestion (Hoffman et al., 2002) has stimulated design of 'smart' matrices able to 'sense' external changes (pH, temperature, humidity) and trigger release of active (drugs) and/or bioactive (protein and genes) compounds (Jeong, Kim, & Bae, 2002). Although applications are less developed, these same properties offer promise for use of biopolymers in packaging materials as stand-alone films (Mohareb & Mittal, 2007; Weber, Haugaard, Festersen, & Bertelsen, 2002) and as thin layers that either carry active compounds to be released into a targeted environment or provide a coating to improve the properties of a base film (Gong, Katsuyama, Kurokawa, & Osada, 2003).

In spite of well-established benefits, biomaterials still suffer some drawbacks that hinder full exploitation. Most widely recognized limitations include mechanical weakness (and thus inability to withstand loads) (Farris, Introzzi, & Piergiovanni, 2009a), water sensitivity (which leads to unwanted matrix failures) (Yao, Liu, Chang, Hsu, & Chen, 2004), and instability under physiological conditions with unpredictable behaviour in long-term applications (Lin et al., 2006). Although different strategies may be pursued to overcome these problems, the

inherent versatility and multifunctionality of such biomolecules offer a valuable opportunity to improve their physicochemical and biochemical properties, thus affording new possibilities for specific applications (Mourya & Inamdar, 2008; Ravi Kumar, 2000). Accordingly, one way to improve the overall performance of bio-based materials is represented by the association of biomolecules of both different origin and chemical characteristics through the development of new methods/techniques, which makes it possible to fully exploit the reactivity of functional groups along the skeleton of biomolecules (Hoare & Kohane, 2008). Protein-polysaccharide pairs, in particular, have great potential to fabricate many structural complexes and coacervates with improved physicochemical properties, exploitable for films/coatings-forming purposes (Turgeon, Schmitt, & Sanchez, 2007; de Kruif & Tuinier, 2001; Wooster & Augustin, 2007; Giancone, Torrieri, Masi, & Michon, 2009). Among the various combinations, low-methoxyl pectin and gelatin have been described as well-suited hydrocolloids for producing simple hydrogels (Liu, Liu, Fishman, & Hicks, 2007; Nikolova, Panchev, & Sainova, 2005; Gilsenan, Richardson, & Morris, 2003). Recently, low-methoxyl pectin and gelatin have also been indicated as valuable candidate to generate new elaborate architectures originating from a multi-step approach (Farris, Schaich, Liu, Piergiovanni, & Yam, 2009b).

This paper provides experimental evidence for formation of new materials from integrated hydrogel networks using gelatin and low-methoxyl pectin as reactive biopolymers. It is documented the qualitative molecular structures as well as some main quantitative physical properties of films generated from sequential combination of hydrogels solutions of low-methoxyl pectin and gelatin. To this purpose, a 2-step approach has been adopted, according to the experimental procedure we proposed recently in the attempt of obtaining new high-performance materials defined as ‘permanent polyion-complex hydrogels’ films (Farris et al., 2009b). The rationale behind the experimental work here presented is thoroughly documented elsewhere (Farris et al., 2009b). Briefly, in a first step, solutions of gelatin and

low-methoxyl pectin are combined to generate a continuous physical co-gel in which the minor component (low-methoxyl pectin) is dispersed through the interstices of the original main network (gelatin). In this mixed matrix, gelatin and pectin interact with each other through electrostatic forces, yielding a reversible physical polyion complex that has better overall performance than either individual polymer. In a second step, the inclusion of glutaraldehyde in this polyion complex chemically crosslinks gelatin, giving rise to a permanent hydrogel complex that improves strength and water-resistance still further. This step is effective because the chemical groups of gelatin involved in the ionic interactions with pectin differ from those forming covalent bonds with glutaraldehyde.

Results demonstrate how progressively increasing the complexity of molecular interactions in biopolymer hydrogels (simple gelatin hydrogels→ physical gelatin-pectin hydrogels→ permanent polyion complexes) can be used creatively to produce flexible films that have tremendously enhanced performances (e.g., strength and moisture resistance). This provides compelling support for using biopolymers from renewable resources to synthesize strong films with desirable properties.

2. Experimental

2.1. Source of materials

Type A, 250 Bloom, pharmaceutical and food grade pigskin gelatin powder (isoelectric point, IEP ~ 9.0): Weishardt International, Grauliet Cedex, France. Low-methoxyl (DE = 7, pK_a ~ 3.5; native pH) pectin: CP Kelco, San Diego, CA. Glycerol (plasticizer): Giomavaro, Brugherio, Italy. Glutaric dialdehyde (25 wt.-% in water): Acros, Morris Plane, NJ. All reagents were used as received, without further purification. All solutions were prepared with Milli-Q water (18.3 MΩ).

2.2. Preparation of the films

Three types of films with 21 wt% total solids but different composition were generated mixing gelatin, pectin, and glycerol in different amount as settled in our previous work (Farris et al., 2009b). Gelatin hydrogels (gel) (native pH ~ 4.5) were prepared by mixing gelatin powder (14 wt.-%) with water containing 7.0 wt.-% glycerol, heating to 60 ± 0.5 °C and holding for 1 h, then cooling to 40.0 ± 0.5 °C. Gelatin-pectin mixed hydrogels (gel-pec) were produced by separately preparing a gelatin (32.5 wt.-%)/glycerol (17.15 wt.-%) water solution, according to the previous procedure, and dissolving 2.56 wt.-% pectin in hot water (90°C) with vigorous stirring (1000 rpm). Then, an aliquot of the pectin solution (40.0 ± 0.5 °C, native pH ~ 4.2) was added to a same aliquot of the gelatin-glycerol water solution (40.0 ± 0.5 °C), to give a final concentration of 13 wt.-% gelatin, 7 wt.-% glycerol and 1 wt.-% pectin. After complete interdispersion of the solutions, the temperature was decreased to 37.0 ± 0.5 °C. At this temperature, glutaraldehyde (0.3 wt.-%) was then added to an aliquot of this solution under thorough and continuous mixing (550 rpm) to crosslink the gelatin and form the third hydrogel (cross).

Once formed, all hydrogels were degassed and spread over the bottom of either Petri dishes (100 mm diameter) or polycarbonate rectangular templates (300 mm length x 150 mm width), depending on the specific successive analysis. Final films were obtained after evaporation of water in a vacuum oven (Model 282, Fisher Scientific, Pittsburgh, PA) at 40.0 ± 0.5 °C for 24 hrs. Crosslinked films were additionally washed several times with Milli-Q water and then air-dried at room temperature for 24 hours. The thicknesses of the final structures, measured to the nearest 0.001 mm with a micrometer (Dialmatic DDI030M, Bowers Metrology, Bradford, UK) at 10 different locations selected randomly, was 100 ± 5 μm.

2.3. Visualization of films structures

2.3.1. Scanning electron microscopy analysis (SEM)

Strips of dry film (5mm wide x 30 mm long) were immersed in 20 ml aliquots of 80 wt.-% ethanol water solution, with several changes. Then 80% ethanol was decanted and replaced with several changes of absolute ethanol. Next, strips were removed from absolute ethanol, quickly blotted dry and immersed in liquid Nitrogen for 5 minutes. The frozen strips were cross fractured manually using cold tweezers and the fractured pieces were thawed in absolute ethanol. Finally, the fragments were critical point dried from liquid CO_2, and the dried fragments were glued to specimen stubs with Duco cement (ITW Performance Polymers, Riviera, FL), sputter-coated with a thin layer of gold and examined with a Quanta 200 FEG scanning electron microscope (FEI Co., Inc., Hillsboro, OR), operated in the high vacuum, secondary electron imaging mode. At least 10 images were collected for each sample.

2.3.2. Atomic force microscopy analysis (AFM)

Small areas (3-4 mm square) of films were cut with surgical scissors, glued to a magnetic sample disk with a carbon adhesive tab (Electron Microscopy Sciences, Hatfield, PA) and mounted on the scanner tube of a Multimode Scanning Probe microscope with a Nanoscope IIIa controller, operated as an atomic force microscope in Tapping mode (Veeco Instruments, Santa Barbara, CA). Small (1.0 and 2.5 micrometer square) areas of the samples were then scanned with the AFM operating in intermittent contact mode using tapping mode etched silicon probes (TESP). The spring constants for these probes were 20-100 N m^{-1} and the nominal tip radius of curvature was 5-10 nm. The cantilever controls, namely drive frequency, amplitude, gains, and amplitude set point ratio (r_{sp}) were adjusted to give height and phase-shift images with the clearest image details.

2.4. Physical properties of the films

2.4.1. Large deformation analysis

Stress-strain curves of 110 mm x 20 mm strips of films equilibrated at 50% relative humidity conditions were collected according to the ASTM procedure (ASTM standard method D882-97) in a typical tensile test using a TAXT2 Stable Micro System texture analyzer (SMS, Surrey, UK) equipped with a 25 kg cell load. The initial grip separation was 100 mm, and the cross-head speed was set at 0.85 mm s^{-1}. Elastic modulus (or Young's modulus, MPa), tensile strength (MPa), and strain at break (%) were automatically calculated by the software Texture Expert version 1.15 (SMS, Surrey, UK). Each type of film was tested by at least ten replicates.

2.4.2. Thermal properties (DSC)

Thermal properties were measured by differential scanning calorimetry (DSC) analysis, using a DSC 823 (Mettler Toledo, Columbus, OH) with a quench-cooling accessory. Aliquots of approximately 10 mg samples previously conditioned (23°C, 50% RH for 2 weeks) were placed in hermetically-sealed aluminium pans to prevent moisture loss during analyses and then heated at 10 °C min^{-1} from 5 °C to 110 °C in an inert environment (100 ml min^{-1} N_2). The first scan was immediately followed by quick cooling to 5 °C at a rate of 40 °C min^{-1} using liquid nitrogen and the second scan was then run. Before taking the measurements, the instrument was calibrated with an indium standard (ΔH of 28.4 J g^{-1} and Tm of 156.6 °C). The glass transition temperature (T_g) of all the samples was determined as the point of inflexion in the base line (second scan) caused by the discontinuity of specific heat capacity of the sample. The helix-coil transition temperature, T_m, also called interchangeable melting or denaturation temperature (Arvanitoyannis, Nakayama, & Aiba, 1998), was measured as the temperature of the endothermic peak (first scan). The value of helix-coil transition enthalpy (ΔH) was assumed derived from the amount of renaturated gelatin during the sol-gel process (Dai,

191 Chen, & Liu, 2005), and was normalized to the sample weight determined immediately before
192 each measurement. Tg, Tm, and ΔH were calculated by the software STAR^e version 9.0
193 (Mettler Toledo, Columbus, OH).

194 *2.4.3. Dynamic mechanical analysis (DMA)*

195 Dynamic mechanical properties (storage modulus – E', and loss modulus – E'') were
196 determined in the tensile mode using a Rheometric Scientific RSA II Solids Analyzer
197 (Rheometric Scientific, Piscataway, NJ) equipped with Orchestrator 6.5.7 software. Samples
198 (38.1 mm long and 5–7 mm wide) were analyzed as described previously (Coffin, & Fishman,
199 1994), using a temperature ramp from -50 to +150°C at a heating rate of 10°C min^{-1}.

200 *2.4.4. Swelling behaviour*

201 To evaluate the water sorption resistance of the gelatin-based films, square pieces of dry
202 samples were weighed (W_i) and then immersed in distilled water at 30°C with shaking (100
203 rpm) for up to 25 hours. Swollen gels were removed from water periodically, blotted dry, and
204 weighed (W_f) to track sorption kinetics. The swelling index (SI) was determined as described
205 by others (Myung et al., 2008):

206 $$SI\ (\%) = [(W_f - W_i) / W_i] \times 100$$

207 Five replicates were analyzed for each time point.

208 *2.4.5. Statistical analysis*

209 Statistical significance of differences in films properties and behaviours was determined from
210 one-way ANOVA using Statgraphics Plus 4.0 software (STSC, Rockville, USA). The mean
211 values, where appropriate, were separated by least significant difference multiple range test at
212 $p \leq 0.05$.

213

214

3. Results and Discussion

3.1. Structural analysis - Microscopy experiments

3.1.1. SEM analysis

More global organization was revealed by scanning electron microscopy. SEM images of frozen-fractured surfaces of gelatin (gel) films showed rough, overlapping layers (10000x magnification, Figure 1, left) at the fracture faces, composed of ropelike aggregates in a relatively ordered arrangement (25000x magnification, Figure 1, right). With the inclusion of pectin, the pattern of topographical features in the fracture faces appears more irregular (Figure 2, left), whereas higher magnification reveals regions with larger features (Figure 2, right). Since the magnification of Figures 1 and 2 are the same, a comparison demonstrates that gelatin is represented by the smaller regions in Figure 2, whereas it is more difficult to ascertain whether the structures that stand out in Figure 2 (the larger domains) are either (1) the pectin, (2) gelatin with increased self-association forced by exclusion from areas with pectin, or (3) gelatin-pectin intertwined complexes. However, supported by previous results (Gilsenan et al., 2003), we believe that the large patches are produced by gelatin-pectin complexes. This is because, under the experimental conditions (i.e., pH = 4.5), the gelatin backbone exhibits an overall positive charge, whereas the carboxyl group along the pectin skeleton are indeed carboxylates. Therefore, due to the addition of pectin, positively charged gelatin and negatively charged pectin would be expected to interact through electrostatic forces between NH_3^+ and COO^- groups. Addition of 0.3 wt% glutaraldehyde produced more evident heterogeneity in the microstructure. In particular, the lumpy structures may represent large groups of polymers (triangles in Figure 3) with a separate phase entrapped within (arrows in Figure 3). The largest domains probably represent glutaraldehyde-mediated protein-polysaccharide interactions (Nikolova et al., 2005). Lately, it has been proved that these aggregates are the evidence of a new crosslinking mechanism of gelatin mediated by

glutaraldehyde. Unlike the established reaction between the carbonyl group of glutaraldehyde and the unprotonated ε-amino groups of lysine to form Schiff bases, it has been proposed that at acidic pH the crosslinking occurs prevalently between the aldehyde groups of the crosslinker and hydroxyl groups of hydroxyproline and hydroxylysine of gelatin (91 and 6.4 residues per 1000 residues in type A gelatin, respectively) to form hemiacetals (Farris, Song, & Huang, 2010), according to the mechanism shown in Figure 4. As we pointed out, it is likely that under the experimental conditions, unprotonated amino groups of gelatin and carbonyl groups of the crosslinker contribute to the formation of new bridges only to a minor extent. The resulting structure can be seen as a tightly packed three-dimensional network composed of a primary entangled phase of chemically-crosslinked gelatin, arranged into fibers that connect and encase a secondary component - pectin, linked to gelatin by ionic interactions. Together these components formed what has been defined as a 'permanent polyion-complex gel' (Farris et al. 2009b).

3.1.2. AFM analysis

In order to understand the structures formed during the gelation process more thoroughly, interfacial gelatin and gelatin-pectin films formed at the air-water interface were also studied using atomic force microscopy (AFM). The AFM 'height' image of films obtained from glycerol-plasticized gelatin (Figure 5, left) well correlates with the molecular network highlighted by Morris and co-workers through the same technique (Morris, Kirby, & Gunning, 1999). Gelatin molecules assemble into aggregates containing short segments of dimensions comparable to those expected for collagen triple helices. The image shows small aggregates typically 200-400 nm in length and about 6 nm in height. The aggregates appear to be clusters of molecules presumably linked by intermolecular triple helix formation. It has been supposed that these fibers are likely to be bundles of triple helices rather than individual helical junction zones (Mackie, Gunning, Ridout, & Morris, 1998). Addition of pectin led to a

265 completely different scenario. Figure 6 (left) revealed that the above-mentioned gelatin
266 clusters disappear giving way to a more homogeneous structure. In particular, it seems that
267 pectin hindered the possibility for gelatin to recover the original triple helix conformation,
268 while promoting the formation of a binary network in which gelatin and pectin are supposed
269 to interact through ionic interactions, as mentioned above. The 'phase' image indeed
270 confirmed the compatibility between the two components, which generated a highly smooth
271 surface, especially in comparison with the 'phase' image drawn from gelatin films (Figure 5,
272 right). As already pointed out (Dautzenberg & Jaeger, 2002), the effect of charge density
273 (which can be manipulated by the pH of the system) on the stability of polyelectrolyte
274 complexes must be kept under control. Therefore, also in our system the charge balance
275 (which is controlled by the polyelectrolytes ratio in the mixed dispersion) between gelatin and
276 pectin plays a pivotal role in order to have a uniformly distributed network. Combining
277 gelatin and pectin in different stoichiometries alters the positive/negative charge balance and
278 hence the extent of associations between these two polyions (Farris et al., 2009b). Our results
279 demonstrate that combining 13 wt.-% of type A 250 Bloom gelatin and 1 wt.-% low methoxyl
280 pectin (DE = 7) at native pH (~ 4.5) generates a physical polyion complex composed of a
281 main gelatin network augmented by additional associations through ionic interactions with
282 pectin, with no evidence of either large domains from self-aggregations or precipitation upon
283 complex formation. However, when the molar excess of one component is too great,
284 segregative interactions occur and the system evolves into two co-existing phases (Gilsenan et
285 al., 2003). This phenomenon is shown in Figure 7 (left) where gelatin domains (the darker
286 regions) are separated from the pectin molecules (the bright 'scrapes'), which in turn are
287 associated through homotypic junctions analogously to a single-component gel. The final
288 result is a rougher topography (Figure 7, right). Finally, AFM images of crosslinked samples
289 are consistent with the results from the SEM analysis. The morphology of the final structure is
290 strongly influenced by the addition of glutaraldehyde, which induced the formation of new

bonds between gelatin molecules especially at intermolecular level (Farris et al., 2010), yielding a more pronounced web-like conformation, with pectin molecules forming part of it (Figure 8, left). At the same time, due to these new domains, the surface topography appears rough and noisy (Figure 8, right).

3.2. Physical properties of films

3.2.1. Large deformation analysis

As shown by Figure 9, the mean stress-strain curves for the three types of films differ from each other, as also confirmed by the results reported in Table 1. The elastic modulus values were calculated for all specimens from the slope of the linear climbing tract of the stress-strain plot within the fixed strain region 0.5% – 1.0%, as visualized in the magnification embedded in Figure 9. The elastic modulus values recorded for the (gel) samples are approximately two and one and half times higher than those obtained for (gel-pec) and (cross) samples, respectively (Table 1). This can be ascribed to the lower degree of crystallinity of (gel-pec) and (cross) samples. Both interactions governed by electrostatic forces and covalent bonds reduced the crystallinity degree of the gelatin main network because close packing of molecules is prevented, thus resulting in lower stiffness of the polymer (Andersson, 2008). Since the slope of the first rising tract of a stress-strain curve gives a measure of the material's stiffness, which is normally assumed to be an indication of the degree of crystallinity (Selke, Culter, & Hernandez, 2004), it can be concluded that the gelatin samples had a higher degree of crystallinity than the other samples. Our results agree with those obtained by Thomazine, Carvalho and Sobral (2005), where gelatin films plasticized with glycerol (55 wt% of gelatin content) had an elastic modulus mean value of 0.41 ± 0.11 MPa. Our results also show how the physical hydrogel solution made by the negatively charged pectin and the positively charged gelatin led to films with tensile strength and elongation at break respectively 26% and

316 24% higher than samples obtained from only gelatin. Addition of glutaraldheyde made it
317 possible to obtain films with still further improved mechanical properties. Presumably,
318 uneven crosslinking occurred during films preparation led to development of new zones in
319 which typical 'irreversible' features (new covalent bonds at both intramolecular and
320 intermolecular level) are dominant compared to the still present 'reversible' domains, in
321 which interactions within and between molecules are mainly governed by weak forces
322 (hydrophobic associations, ionic interactions, or hydrogen bonding) and/or physical
323 entanglement. As can be seen from Table 1, crosslinking increased both tensile strength and
324 elongation at break, though the latter was not statistically different from samples obtained
325 from the gelatin-pectin physical hydrogel solution. In order to substantiate the positive role of
326 the electrostatic interactions between gelatin and pectin, we also performed the tensile test on
327 samples obtained from only gelatin crosslinked with glutaraldehyde. These films had elastic
328 modulus, tensile strength and elongation at break values of 0.22 ± 0.05 MPa, 14.01 ± 2.36
329 MPa and 149.3 ± 8.09%, respectively. These results suggest that the best performance of
330 crosslinked gelatin-pectin films can be presumably ascribed to the additional effect due to the
331 electrostatic interactions between the oppositely charged functional groups of the two
332 biomacromolecules.

333 *3.2.2. Thermal properties (DSC)*

334 Figure 10 shows the differential scanning calorimetry (DSC) traces obtained from the
335 first scan of pure gelatin, gelatin-pectin, and gelatin-pectin films crosslinked using
336 glutaraldehyde. All traces display the classical thermal behaviour of gelatin samples, with the
337 first drop of the curve related to the glass transition, followed by an endothermic peak
338 associated with the helix to coil transition. In the second heating scan, only the glass transition
339 is evident (a typical heating-cooling-heating DSC trace for non-crosslinked glycerol-
340 plasticized gelatin samples equilibrated at 50% relative humidity is displayed in Figure 11).

This is due to the disruption of the microcrystalline domains during the first heating cycle. From Figure 10 it can be observed how (gel) and (gel-pec) samples provided very similar traces, contrary to (cross) samples, which led to a curve with an anticipated and less pronounced peak. More specifically, (gel) samples had T_g = 50.53 ± 0.6 °C, T_m = 59.45 ± 0.3 °C, and ΔH = 10.9 ± 0.3 J g^{-1}. (Gel-pec) samples were characterized by T_g = 51.23 ± 0.7 °C, T_m = 59.23 ± 0.2 °C, and ΔH = 9.4 ± 0.5 J g^{-1}. Finally, crosslinked samples yielded T_g = 44.78 ± 0.6 °C, T_m = 50.37 ± 0.4 °C, and ΔH = 3.2 ± 0.4 J g^{-1}. The overall lower values for crosslinked samples can be explained by taking into consideration two different effects. Firstly, the appearance of the endothermic peak in a DSC curve is normally due to the breakage of hydrogen bonds. Conversely, when a crosslinked network structure is involved, a small or negligible endothermic peak is expected. Therefore, the decrease in the helix-to-coil enthalpy values (ΔH) when using glutaraldehyde has to be attributed to an increase in the extent of crosslinked network formation which breaks exothermically. Secondly, the simultaneous lower T_g of (cross) samples can be explained by hypothesizing an 'inhibition effect' exerted by the crosslinker, which prevented the recovery of the structurally-ordered microcrystalline domains (the so called microcrystallites), to the advantage of a more amorphous final molecular structure.

3.2.3. Dynamic mechanical analysis (DMA)

A dynamic mechanical analysis was performed on selected samples obtained from hydrogel solutions containing only gelatin, gelatin and pectin, and gelatin and pectin with glutaraldehyde. The storage modulus curves (E') are shown in Figure 12a, while the loss modulus curves (E") are shown in Figure 12b. Both the storage modulus and loss modulus curves for the gelatin-only samples had significantly lower values than did the curves for the other two samples throughout the entire temperature range studied. Two transitions were present in all three samples. The first was a peak in the loss modulus curve centered at

approximately -56°C. This is likely due to a glass to rubber transition (T_g) associated with soft blocks containing mainly R-amino acids. A second peak near 50°C may be related to a second glass transition of rigid gelatin blocks composed of sequences predominately made up of the amino acids proline and hydroxyproline (Chiellini, Cinelli, Grillo Fernandes, El-Refaie, & Lazzeri, 2001). The addition of pectin to the gelatin increased both the storage modulus and loss modulus of the material. Above -60°C, crosslinking had little or no effect on mechanical properties, although a very slight decrease in modulus there may have resulted below this temperature. The results of the DMA analyses show some confirmation of what was previously shown in the DSC experiment. In particular, there are no changes in thermal stability when the gelatin hydrogel is modified by the addition of pectin, and then further modified by reaction with glutaraldehyde.

3.2.4. Swelling behaviour

Results from swelling experiments are summarized in Figure 13. Curves obtained by plotting the swelling index versus time indicate how water absorption was markedly higher for (gel) samples, whereas differences between (gel-pec) and (cross) samples were negligible up to 120 minutes. In addition, (gel) samples gained water throughout the experiment, whereas both uncrosslinked and crosslinked gelatin-pectin films reached a quite stable equilibrium swelling level after approximately 240 minutes. Moreover, the experiments were stopped after 25 hours due to the impossibility of taking gelatin samples out of the stirring jars because of their complete disintegration. Conversely, it was still possible to handle (gel-pec) and (cross) samples even after 25 hours. It is noticeable that at that time, (gel-pec) pieces of samples cannot sustain any kind of stress without failure, while it was possible to stretch (cross) samples without rupture, somehow confirming the reversible nature of the (gel-pec) samples and the permanent feature of crosslinked samples. These results confirm the benefits arising from the addition of pectin first and crosslinker later. Exploiting electrostatic

391 interactions between the two biomacromolecules made it possible to achieve a dramatic
392 decrease in the ultimate swelling ratio (300% versus 1950% of gelatin samples). After all,
393 electrostatic self-assembly is a widely established route to generate supramolecular structures
394 with enhanced properties (Grohn, 2008). Presumably, electrostatic interactions between
395 gelatin and pectin hinder penetration of water molecules, which will take a longer time to
396 compete for the same hydrophilic sites along the molecular skeleton of the two biomolecules.
397 Inducing new permanent bonds through glutaraldehyde further enhanced this trend. Indeed,
398 films crosslinked with only 0.3 wt.-% glutaraldehyde swelled approximately ten times less
399 than uncrosslinked gelatin samples (215% versus 1950%) after 25 hours, indicating how the
400 irreversible attribute of the hydrogel solution initially used to produce the films provided a
401 greater water resistance. As also suggested by AFM images (Figure 7), it is likely that the
402 addition of the crosslinker led to a heterogeneous molecular arrangement, due to the presence
403 of domains with an uneven degree of crosslinking, which determines the simultaneous
404 presence of crosslinked undissolvable patches together with zones in which the typical
405 'reversible' features are still dominant. These features are responsible for the occurred
406 swelling, which in turn strictly depends on the extent of the crosslinking. As a consequence, a
407 slightly higher concentration of glutaraldehyde within a certain limit should afford additional
408 resistance to swelling, without jeopardizing the film-making process (Bigi, Cojazzi,
409 Panzavolta, Rubini, & Roveri, 2001).
410 Finally, the role of glycerol in the ultimate water resistance property of the obtained films
411 should not be underestimated. Glycerol was here used as a plasticizer, which provides films
412 with improved mechanical properties especially in terms of flexibility. However, both the
413 small size and polar nature of this molecule influence the physical structure of the
414 biopolymers (increasing the free volume between adjacent molecules) as well as their affinity
415 to water. Therefore, the tendency of water sorption becomes even more significant.

Depending on the specific application, either replacing glycerol with other molecules or removing it from the starting formulation may provide desirable benefits.

4. Conclusions

The results arising from our investigation showed the importance of developing a proper hydrogel solution for producing ultimate films with improved overall properties. In particular, microscopy analyses corroborate the hypothesis that the addition of pectin to gelatin according to a well defined ratio leads to a composite network in which the protein and the polysaccharide interact with each other through electrostatic forces. It afforded structures with improved mechanical and water resistance properties, which could be profitably exploited for manufacturing special materials, in order to replace some of the commercial solutions currently used. In addition, crosslinking mediated by glutaraldehyde promoted the formation of covalent bonds between gelatin molecules, without interfering with the previously mentioned physical interactions, and allowing the formation of an interconnected gelatin web with the pectin network dispersed inside. Physical characterization of gelatin-based films indirectly supports our findings. The molecular arrangement we propose indeed justifies the increased performance of the obtained structures, which demonstrates the capability of withstand high loads simultaneously to a great elongation, and good water resistance as well (films swelled, but never dissolved nor disintegrated).

Acknowledgements: we are thankful to Dr. *D. Coffin* and *G. Bao* for technical and scientific assistance.

441 **References**

442 Andersson, C. (2008). New ways to enhance the functionality of paperboard by surface
443 treatment - a review. *Packaging Technology and Science*, 21 (6), 339-373.

444 Arvanitoyannis, I.S., Nakayama, A., & Aiba, S. (1998). Chitosan and gelatin based edible
445 films: state diagrams, mechanical and permeation properties. *Carbohydrate Polymers*, 37 (4),
446 371-382.

447 ASTM 1997. Designation D 882-97: Standard test method for tensile properties of thin plastic
448 sheeting. Annual Book of ASTM Standards; American Society for Testing and Materials:
449 Philadelphia, 1997, p 159.

450 Bigi, A., Cojazzi, G., Panzavolta, S., Rubini, K., & Roveri, N. (2001). Mechanical and
451 thermal properties of gelatin films at different degrees of glutaraldehyde crosslinking.
452 *Biomaterials*, 22 (8), 763-768.

453 Chiellini, E., Cinelli, P., Grillo Fernandes, E., El-Refaie, S.K., & Lazzeri, A. (2001). Gelatin-
454 based blends and composites. Morphological and thermal mechanical characterization.
455 *Biomacromolecules*, 2 (3), 806-811.

456 Coffin, D.R., & Fishman, M.L. (1994). Physical and mechanical properties of highly
457 plasticized pectin/starch films. *Journal of Applied Polymer Science*, 54 (9), 1311-1320.

458 Dai, C.A., Chen, Y.F., & Liu, M.W. (2006). Thermal properties measurements of renatured
459 gelatin using conventional and temperature modulated differential scanning calorimetry.
460 *Journal of Applied Polymer Science*, 99 (4), 1795-1801.

461 Dautzenberg, H., & Jaeger, W. (2002). Effect of charge density on the formation and salt
462 stability of polyelectrolyte complexes. *Macromolecular Chemistry and Physics*, 203 (14),
463 2095-2102.

De Kruif, G., & Tuinier, R. (2001). Polysaccharide protein interactions. *Food Hydrocolloids*, 15 (4-6), 555-563.

Farris, S., Introzzi, L., & Piergiovanni, L. (2009a). Evaluation of a bio-coating as a solution to improve barrier, friction and optical properties of plastic films. *Packaging Technology and Science*, 22 (2), 69-83.

Farris, S., Schaich, K.M., Liu, L., Piergiovanni, L., & Yam, K.L. (2009b). Development of polyion-complex hydrogels as an alternative approach for the production of bio-based polymers for food packaging applications: a review. *Trends in Food Science and Technology*, 20 (8), 316-332.

Farris, S., Song, J., & Huang, Q. (2010). Alternative reaction mechanism for the cross-linking of gelatin with glutaraldehyde. *Journal of Agricultural and Food Chemistry*, 58 (2), 998-1003.

Ghaffari, A., Navaee, K., Oskoui, M., Bayati, K., & Rafiee-Tehrani, M. (2007). Preparation and characterization of free mixed-film of pectin/chitosan/Eudragit® RS intended for sigmoidal drug delivery. *European Journal of Pharmaceutics and Biopharmaceutics*, 67 (1), 175-186.

Giancone, T., Torrieri, E., Masi, P., & Michon, C. (2009). Protein–polysaccharide interactions: phase behaviour of pectin–soy flour mixture. *Food Hydrocolloids*, 23 (5), 1263-1269.

Gilsenan, P.M., Richardson, R.K., & Morris, E.R. (2003). Associative and segregative interactions between gelatin and low-methoxy pectin: Part 1. Associative interactions in the absence of Ca^{2+}. *Food Hydrocolloids*, 17 (6), 723-737.

Gong, J.P., Katsuyama, Y., Kurokawa, T., & Osada, Y. (2003). Double-network hydrogels with extremely high mechanical strength. *Advanced Materials*, 15 (14), 1155-1158.

Gröhn, F. (2008). Electrostatic self-assembly as route to supramolecular structures. *Macromolecular Chemistry and Physics*, 209 (22), 2295-2301.

Hoare, T.R., & Kohane, D.S. (2008). Hydrogels in drug delivery: progress and challenges. *Polymer*, 49 (8), 1993-2007.

Hoffman, A.S., Stayton, P.S., Press, O., Murthy, N., Lackey, C.A., Cheung, C., Black, F., Campbell, J., Fausto, N., Kyriakides, T.R., & Bornstein, P. (2002). Design of smart polymers that can direct intracellular drug delivery. *Polymers for Advanced Technologies*, 13 (10), 992-999.

Jaklenec, A., Wan, E., Murray, M.E., & Mathiowitz, E. (2008). Novel scaffolds fabricated from protein-loaded microspheres for tissue engineering. *Biomaterials*, 29 (2), 185-192.

Jeong, B., Kim, S.W., & Bae, Y.H. (2002). Thermosensitive sol–gel reversible hydrogels. *Advanced Drug. Delivery Reviews*, 54 (1), 37-51.

Khademhosseini, A., & Langer, R. (2007). Microengineered hydrogels for tissue engineering. *Biomaterials*, 28 (34), 5087-5092.

Kurisawa, M., & Yui, N. (1998). Gelatin/dextran intelligent hydrogels for drug delivery: dual-stimuli-responsive degradation in relation to miscibility in interpenetrating polymer networks. *Macromolecular Chemistry and Physics*, 199 (8), 1547-1554.

Lai, J.Y., Lu, P.L., Chen, K.H., Tabata Y., & Hsiue, G.H. (2006). Effect of charge and molecular weight on the functionality of gelatin carriers for corneal endothelial cell therapy. *Biomacromolecules*, 7 (6), 1836-1844.

508 Lin, C.C., & Metters, A.T. (2006). Hydrogels in controlled release formulations: network
509 design and mathematical modeling. *Advanced Drug Delivery Reviews*, 58 (12-13), 1379-
510 1408.

511 Liu, L., Liu, C.K., Fishman, M.L., & Hicks, K.B. (2007). Composite films from pectin and
512 fish skin gelatin or soybean flour protein. *Journal of Agricultural and Food Chemistry*, 55 (6),
513 2349-2355.

514 Mackie, A.R., Gunning, A.P., Ridout, M.J., & Morris, V.J. (1998). Gelation of gelatin
515 observation in the bulk and at the air–water interface. *Biopolymers*, 46 (4), 245-252.

516 Mohareb, E., & Mittal, G.S. (2007). Formulation and process conditions for
517 biodegradable/edible soy-based packaging trays. *Packaging Technology and Science*, 20 (1),
518 1-15.

519 Morris, V.J., Kirby, A.R., & Gunning, A.P. (1999). Using atomic force microscopy to probe
520 food biopolymer functionality. *Scanning*, 21 (5), 287-292.

521 Mourya, V.K., & Inamdar, N.N. (2008). Chitosan-modifications and applications:
522 Opportunities galore. *Reactive and Functional Polymers*, 68 (6), 1013-1051.

523 Myung, D., Waters, D., Wiseman, M., Duhamel, P.-E., Noolandi, J., Ta, C.N., & Frank, C.W.
524 (2008). Progress in the development of interpenetrating polymer network hydrogels. *Polymers*
525 *for Advanced Technologies*, 19 (6), 647-657.

526 Nikolova, K., Panchev, I., & Sainova, S. (2005). Optical characteristics of biopolymer films
527 from pectin and gelatin. *Journal of Optoelectronics and Advanced Materials*, 7 (3), 1439-
528 1444.

529 Ong, S.Y., Wu, J., Moochhala, S.M., Tan, M.H., & Lu, J. (2008). Development of a chitosan-
530 based wound dressing with improved hemostatic and antimicrobial properties. *Biomaterials*,
531 29 (32), 4323-4332.

532 Ravi Kumar, M.N.V. (2000). A review of chitin and chitosan applications. *Reactive and*
533 *Functional Polymers*, 46 (1), 1-27.

534 Selke, S.E.M., Culter, J.D., & Hernandez, R.J. (2004). *Plastics Packaging: properties,*
535 *processing, applications, and regulations*. Munich: Hanser Carl.

536 Skotak, M., Leonov, A. P., Larsen, G., Noriega, S., & Subramanian, A. (2008). Biocompatible
537 and biodegradable ultrafine fibrillar scaffold materials for tissue engineering by facile grafting
538 of l-lactide onto chitosan. *Biomacromolecules*, 9 (7), 1902-1908.

539 Tharanathan, R.N. (2003). Biodegradable films and composite coatings: past, present and
540 future. *Trends in Food Science & Technology*, 14 (3), 71-78.

541 Thomazine, M., Carvalho, R.A., & Sobral, J.A.P. (2005). Physical properties of gelatin films
542 plasticized by blends of glycerol and sorbitol. *Journal of Food Science*, 70 (3), 172-176.

543 Turgeon, S.L., Schmitt, C., & Sanchez, C. (2007). Protein–polysaccharide complexes and
544 coacervates. *Current Opinion in Colloid & Interface Science*, 12 (4-5), 166-178.

545 Weber, C.J., Haugaard, V., Festersen, R., & Bertelsen, G. (2002). Production and applications
546 of biobased packaging materials for the food industry. *Food Additives and Contaminants*, 19
547 (s), 172-177.

548 Wei, X., Sun, N., Wu, B., Yin, C., & Wu, W. (2006). Sigmoidal release of indomethacin from
549 pectin matrix tablets: Effect of in situ crosslinking by calcium cations. *International Journal*
550 *of Pharmaceutics*, 318 (1-2), 132-138.

Wooster, T.J., & Augustin, M.A. (2007). Rheology of whey protein–dextran conjugate films at the air/water interface. *Food Hydrocolloids*, 21 (7), 1072-1080.

Yao, C.H., Liu, B.S., Chang, C.J., Hsu, S.H., & Chen, Y.S. (2004). Preparation of networks of gelatin and genipin as degradable biomaterials. *Materials Chemistry and Physics*, 83 (2-3), 204-208.

Figure captions

Figure 1. SEM photograph at two different magnifications (10000x – left, and 25000x - right) of frozen-fractured gelatin films plasticized with glycerol (gelatin concentration: 14 wt.-%; glycerol concentration: 7 wt.-%; pH of the hydrogel solution: ~ 4.5).

Figure 2. SEM photograph at two different magnifications (10000x – left, and 25000x - right) of frozen-fractured gelatin-pectin films plasticized with glycerol (gelatin concentration: 13 wt.-%; pectin concentration: 1 wt.-%; glycerol concentration: 7 wt.-%; pH of the hydrogel solution: ~ 4.4).

Figure 3. SEM photograph at two different magnifications (10000x – left, and 25000x - right) of frozen-fractured gelatin-pectin films plasticized with glycerol and crosslinked with glutaraldehyde (gelatin concentration: 13 wt.-%; pectin concentration: 1 wt.-%; glycerol concentration: 7 wt.-%; glutaraldehyde concentration: 0.3%; pH of the hydrogel solution: ~ 4.4).

Figure 4. Mechanism for the crosslinking reaction of gelatin by glutaraldehyde at acidic pH values.

Figure 5. Matching images of (A) height and (B) phase-shift of a gelatin films plasticized with glycerol (gelatin concentration: 14 wt.-%; glycerol concentration: 7 wt.-%; pH of the hydrogel solution: ~ 4.5). The thin clefts or depressions in the surface of the sample in (A) correspond to gelatin triple helix aggregations.

Figure 6. Matching images of (A) height and (B) phase-shift of a film made from a starting glycerol-plasticized gelatin and pectin polyion complex hydrogel solution (gelatin concentration: 13 wt.-%; pectin concentration: 1 wt.-%; glycerol concentration: 7 wt.-%; pH of the hydrogel solution: ~ 4.4).

Figure 7. Matching images of (A) height and (B) phase-shift of a film made from a starting glycerol-plasticized gelatin and pectin polyion complex hydrogel solution with an excess of pectin (gelatin concentration: 10 wt.-%; pectin concentration: 4 wt.-%; glycerol concentration: 7 wt.-%; pH of the hydrogel solution: ~ 4.3). Dark domains are gelatin associations, whereas the bright 'scrapes' are pectin clusters.

Figure 8. Matching images of (A) height and (B) phase-shift of a film made from a starting glycerol-plasticized gelatin and pectin polyion complex hydrogel solution crosslinked with glutaraldehyde (gelatin concentration: 13 wt.-%; pectin concentration: 1 wt.-%; glycerol concentration: 7 wt.-%; glutaraldehyde concentration: 0.3 wt.-%; pH of the hydrogel solution: ~ 4.4). Crosslinked patches appear as a dense web.

Figure 9. Tensile stress-strain curves of gelatin (14 wt.-%), gelatin-pectin (13 wt.-% and 1 wt.-%, respectively), and gelatin-pectin films crosslinked with glutaraldehyde (0.3 wt.-%). All films were plasticized with glycerol (7 wt.-%). Experimental testing conditions: 23 ± 0.5 °C, 50 ± 2.0 % relative humidity.

Figure 10. DSC traces (first scan) of pure gelatin, gelatin-pectin, and gelatin-pectin crosslinked films equilibrated at 23 ± 0.5 °C and 50 ± 2.0 % relative humidity before analysis.

Figure 11. A typical heating-cooling-heating DSC trace for a glycerol-plasticized gelatin film (gelatin: 14 wt-%; glycerol: 7 wt-%) equilibrated at 50% relative humidity.

Figure 12. Storage modulus - E′ (a) and loss mosulus - E″ (b) of gelatin (14 wt.-%), gelatin-pectin (13 wt.-% and 1 wt.-%, respectively), and gelatin-pectin films crosslinked with glutaraldehyde (0.3 wt.-%). All films were plasticized with glycerol (7 wt.-%).

Figure 13. Swelling index evolution of gelatin (14 wt.-%), gelatin-pectin (13 wt.-% and 1 wt.-%, respectively), and gelatin-pectin films crosslinked with glutaraldehyde (0.3 wt.-%) up to 25 hours immersion in distilled water (30°C, 100 rpm). All films were plasticized with glycerol (7 wt.-%).

Figure 1

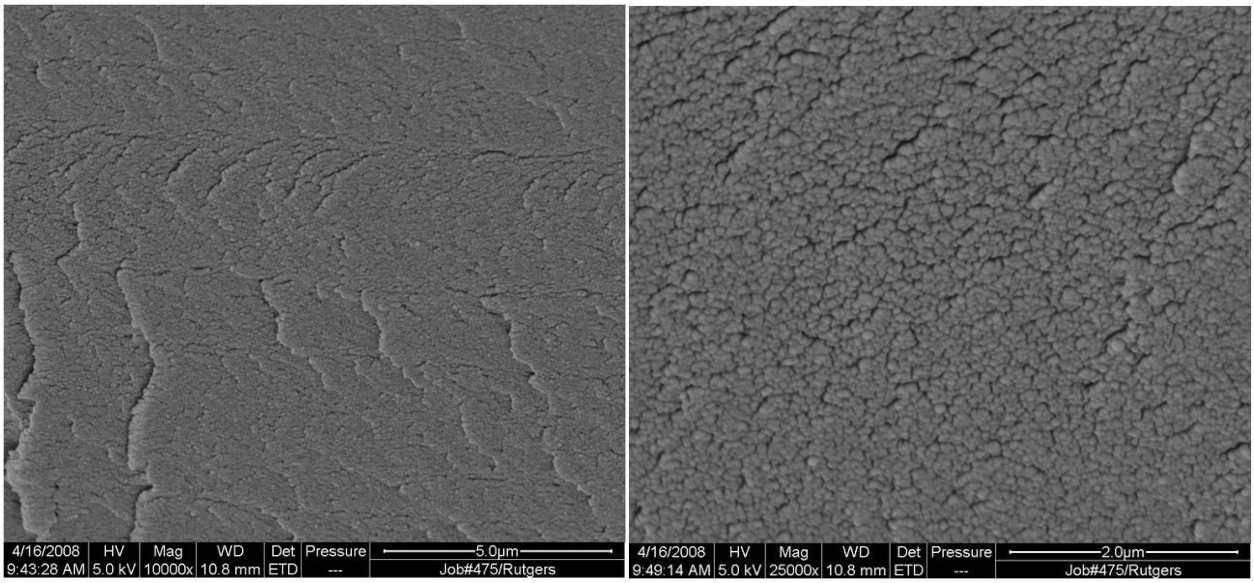
4/16/2008 | HV | Mag | WD | Det | Pressure | 5.0µm
9:43:28 AM | 5.0 kV | 10000x | 10.8 mm | ETD | --- | Job#475/Rutgers
4/16/2008 | HV | Mag | WD | Det | Pressure | 2.0µm
9:49:14 AM | 5.0 kV | 25000x | 10.8 mm | ETD | --- | Job#475/Rutgers

Figure 2

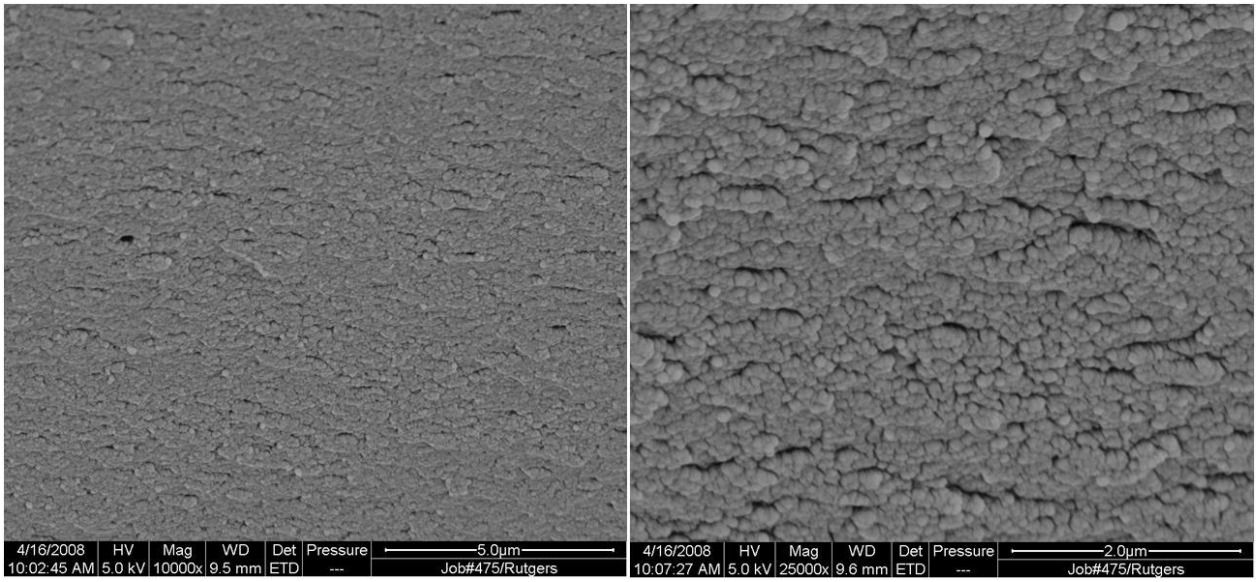
4/16/2008 | HV | Mag | WD | Det | Pressure | 5.0µm
10:02:45 AM | 5.0 kV | 10000x | 9.5 mm | ETD | --- | Job#475/Rutgers
4/16/2008 | HV | Mag | WD | Det | Pressure | 2.0µm
10:07:27 AM | 5.0 kV | 25000x | 9.6 mm | ETD | --- | Job#475/Rutgers

Figure 3

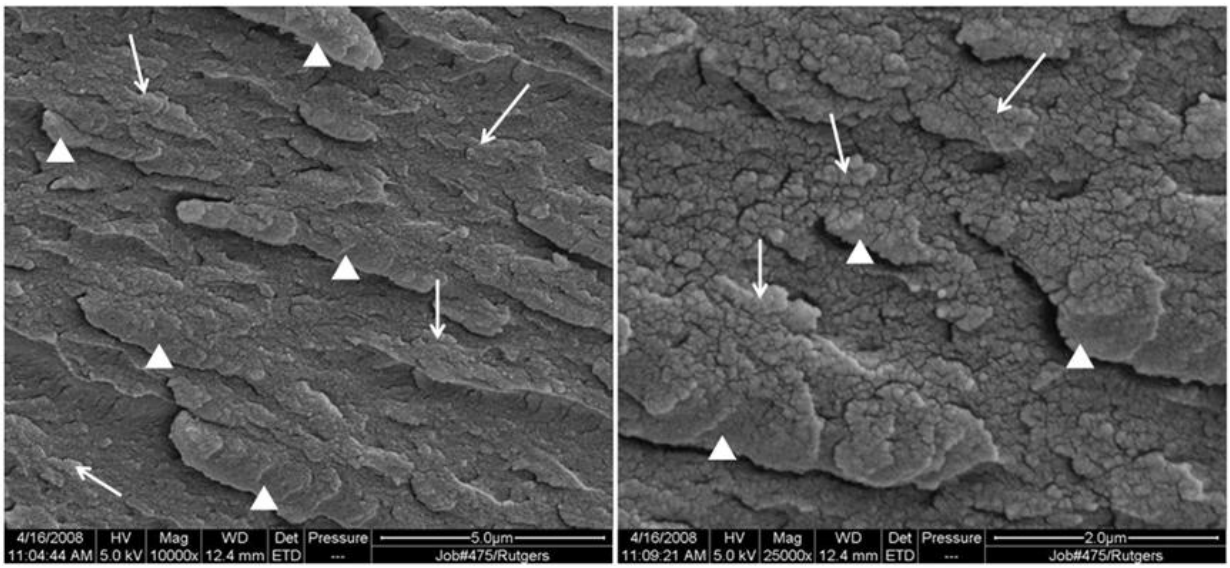
4/16/2008 11:04:44 AM
HV 5.0 kV
Mag 10000x
WD 12.4 mm
Det ETD
Pressure ---
5.0µm
Job#475/Rutgers
4/16/2008 11:09:21 AM
HV 5.0 kV
Mag 25000x
WD 12.4 mm
Det ETD
Pressure ---
2.0µm
Job#475/Rutgers

Figure 4

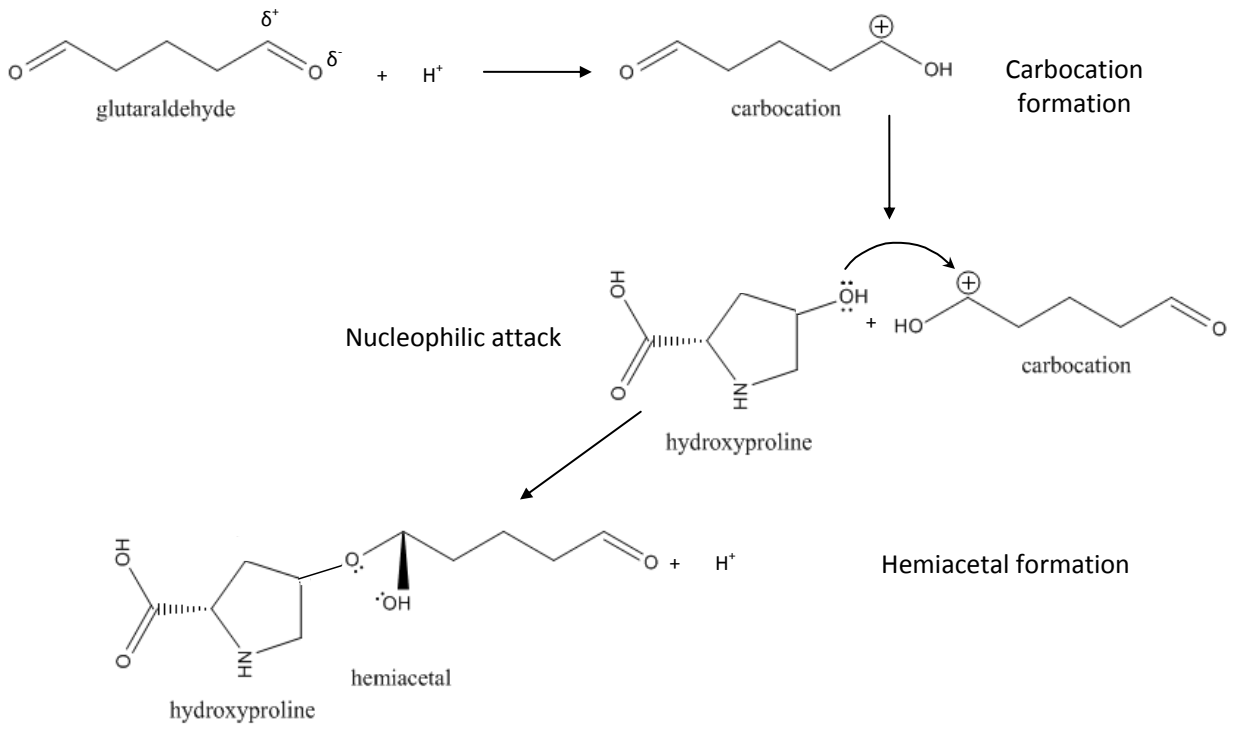
δ+
δ-
O
O
+ H+
glutaraldehyde
carbocation
OH
Carbocation formation
Nucleophilic attack
OH
O
HN
OH
+
HO
carbocation
hydroxyproline
OH
O
HN
O
O
OH
+ H+
hemiacetal
hydroxyproline
Hemiacetal formation

Figure 5

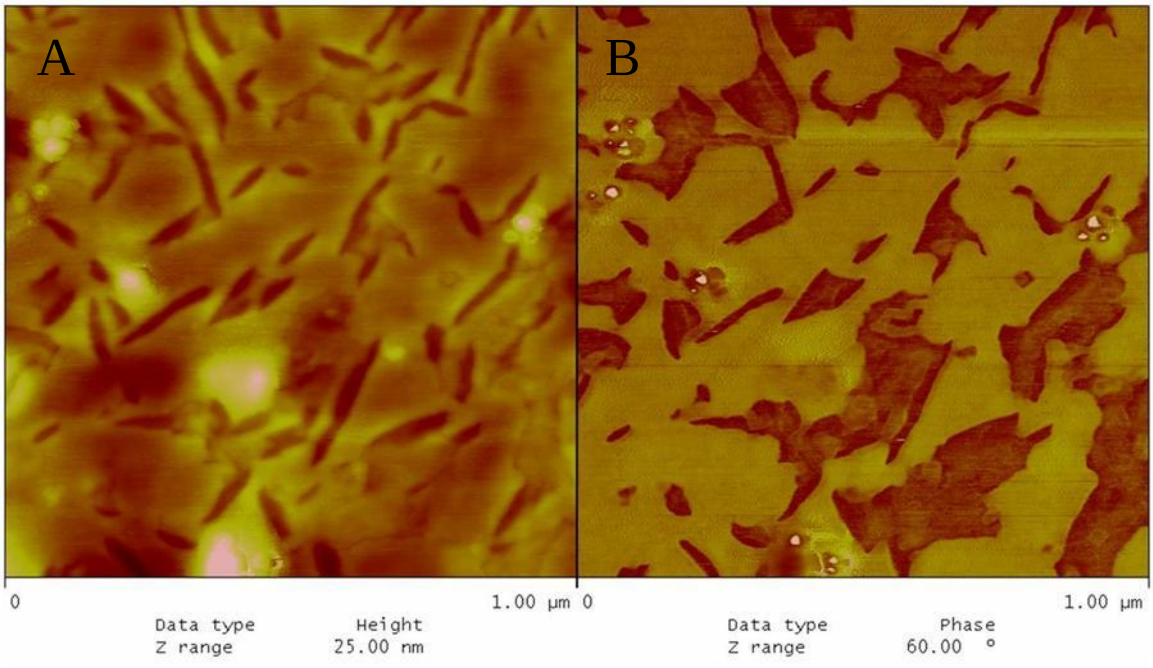
A
B
0
1.00 µm
Data type
Height
Z range
25.00 nm
0
1.00 µm
Data type
Phase
Z range
60.00 °

Figure 6

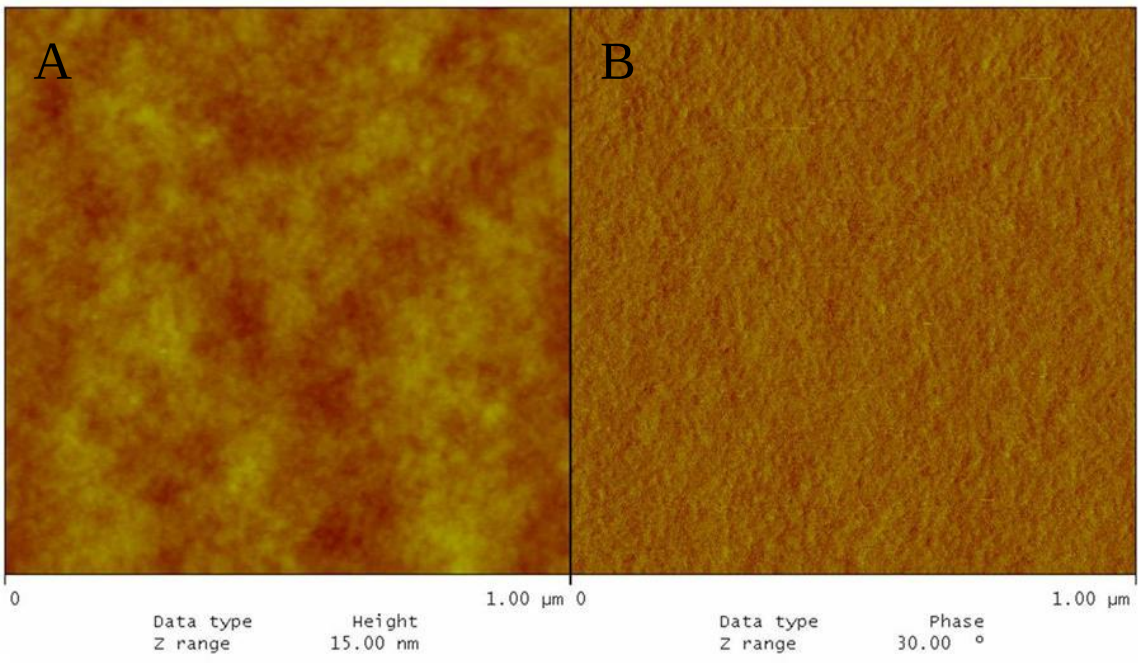
A
B
0
1.00 µm
Data type
Height
Z range
15.00 nm
0
1.00 µm
Data type
Phase
Z range
30.00 °

Figure 7

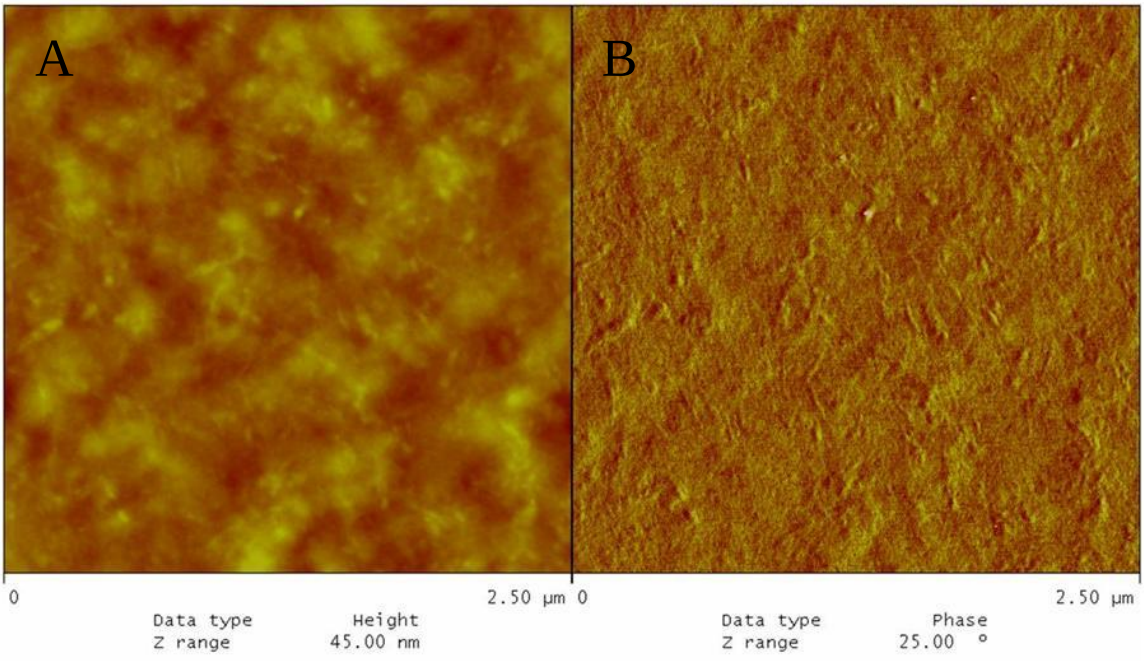
A
B
0
2.50 µm
Data type
Height
Z range
45.00 nm
0
2.50 µm
Data type
Phase
Z range
25.00 °

Figure 8

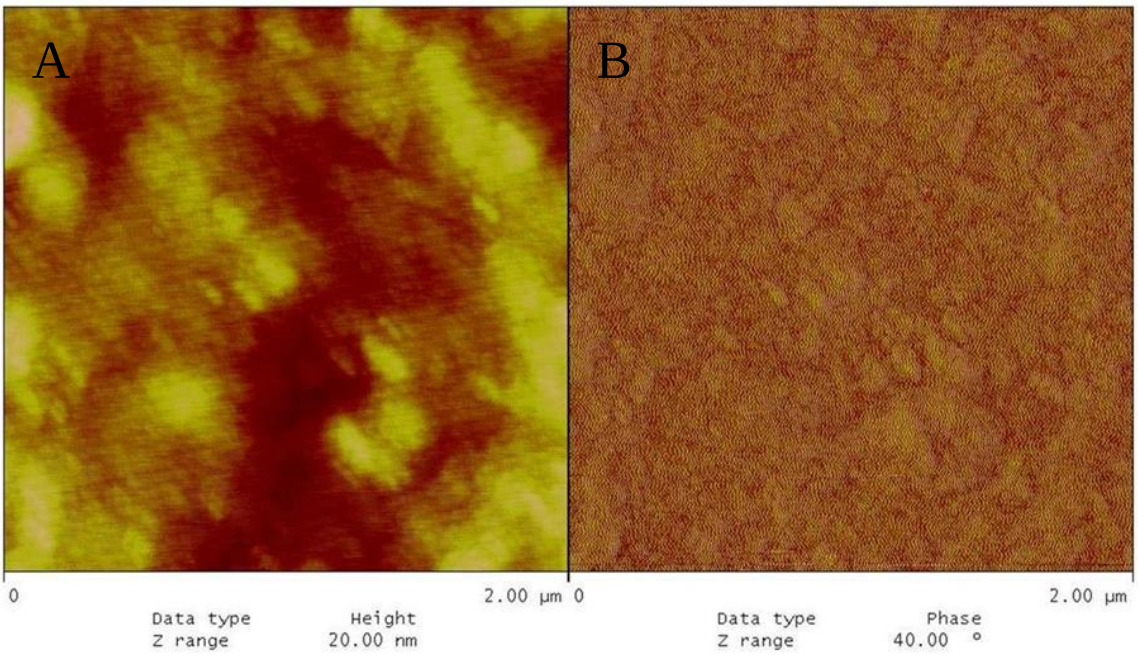
A
B
0
2.00 µm
Data type
Height
Z range
20.00 nm
0
2.00 µm
Data type
Phase
Z range
40.00 °

Figure 9

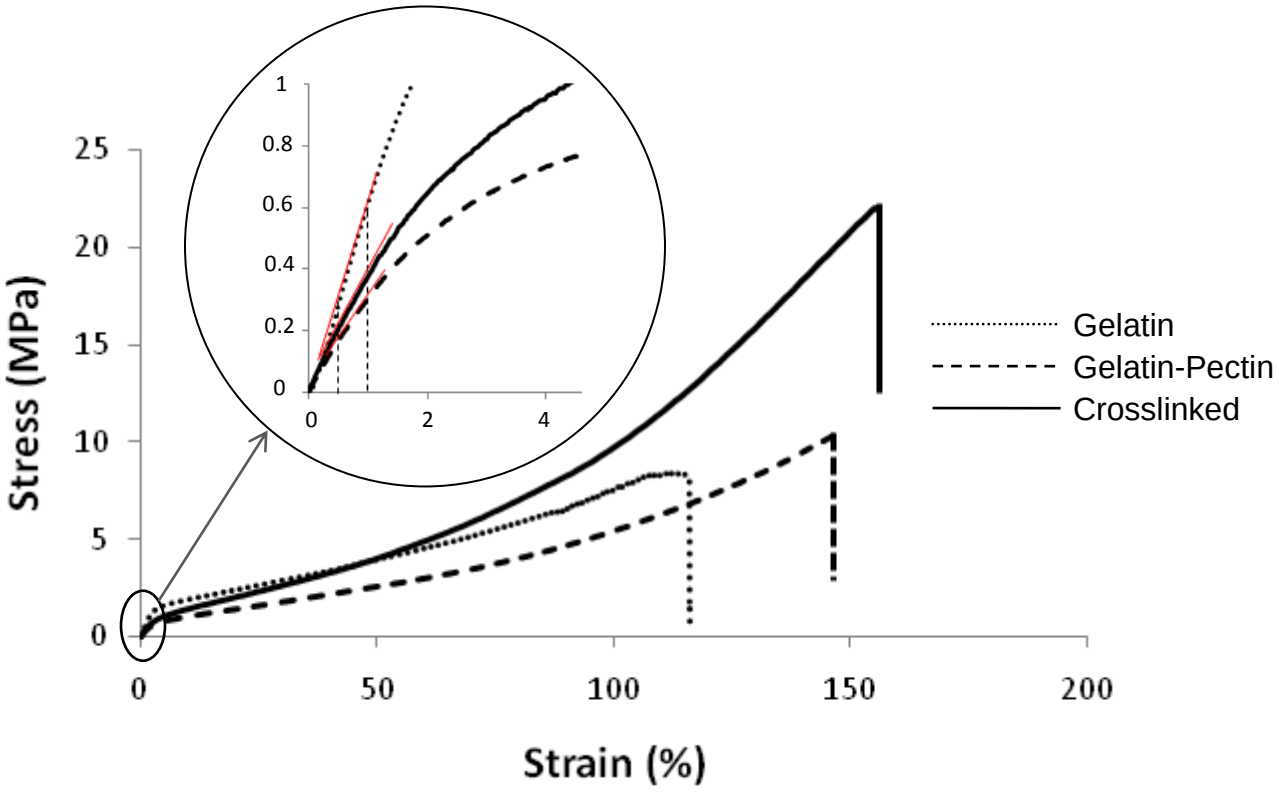
Stress (MPa)
Strain (%)
0
5
10
15
20
25
0
50
100
150
200
1
0.8
0.6
0.4
0.2
0
0
2
4
Gelatin
Gelatin-Pectin
Crosslinked

Figure 10

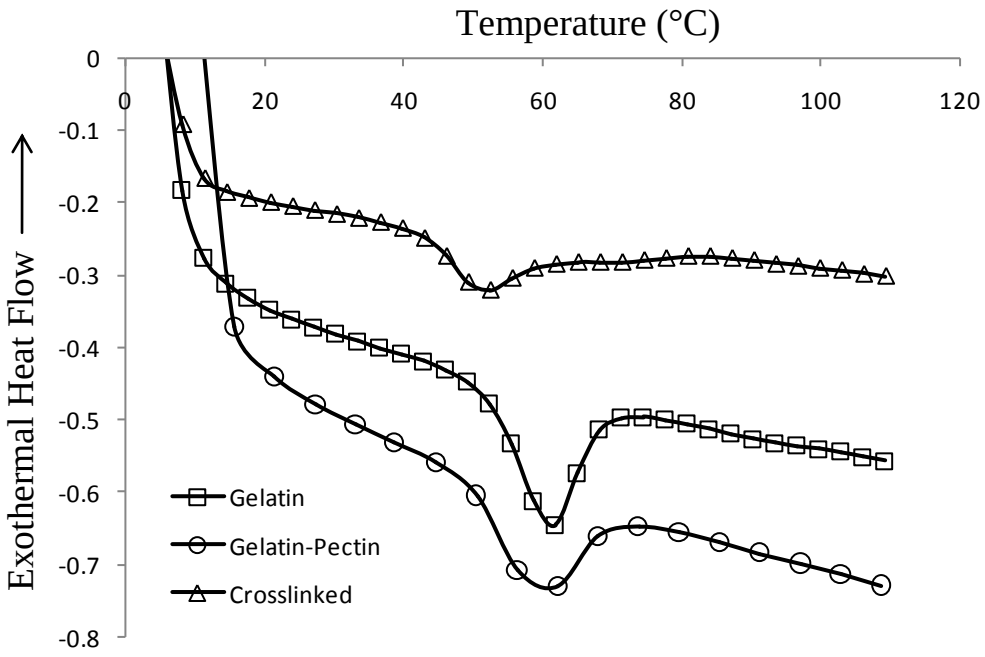
Temperature (°C)
Exothermal Heat Flow
0
-0.1
-0.2
-0.3
-0.4
-0.5
-0.6
-0.7
-0.8
0
20
40
60
80
100
120
Gelatin
Gelatin-Pectin
Crosslinked

Figure 11

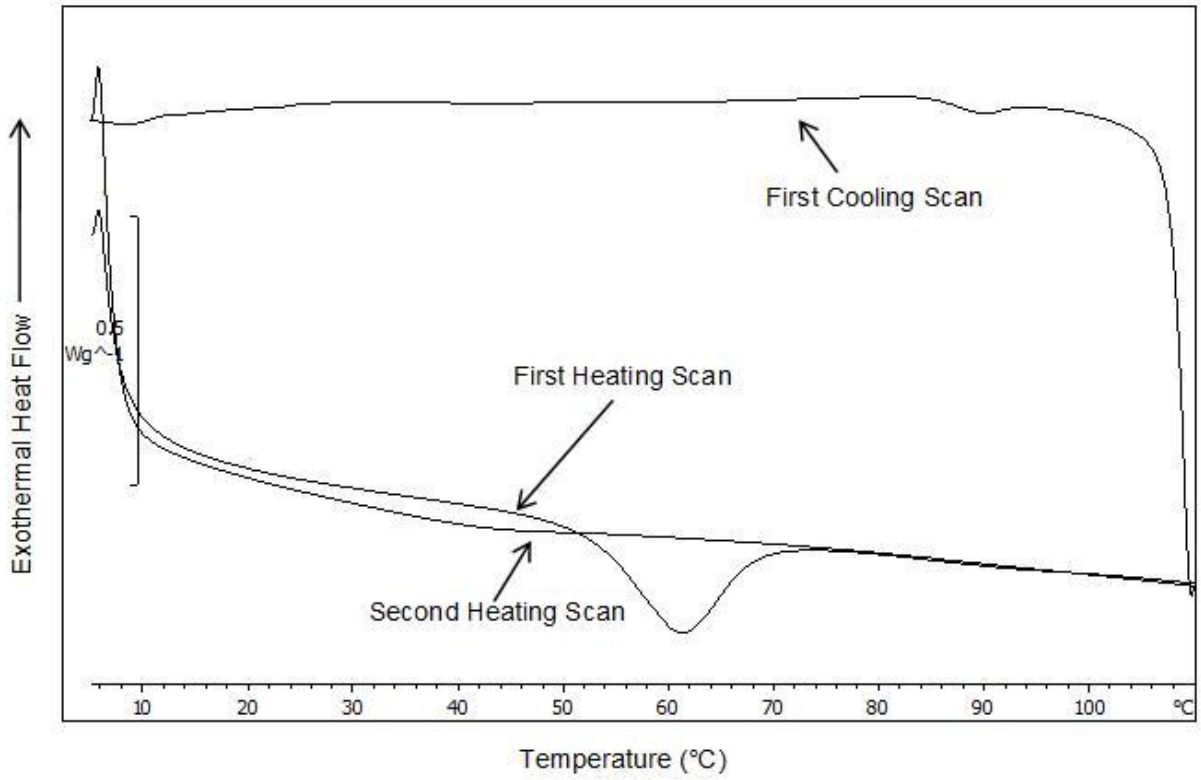
First Cooling Scan
First Heating Scan
Second Heating Scan
Exothermal Heat Flow
Temperature (°C)
10
20
30
40
50
60
70
80
90
100
°C

Figure 12

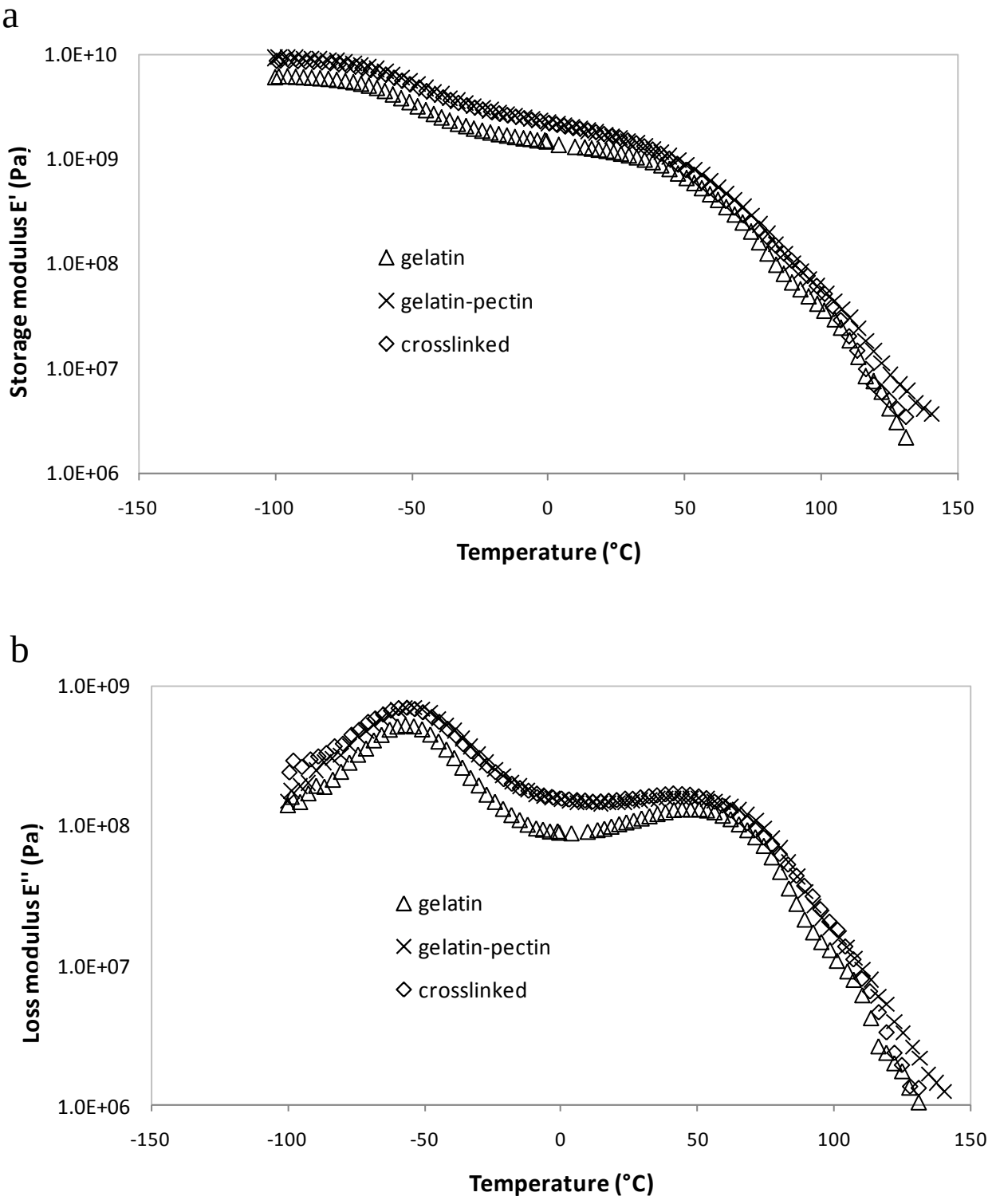
a
1.0E+10
1.0E+09
1.0E+08
1.0E+07
1.0E+06
Storage modulus E' (Pa)
gelatin
gelatin-pectin
crosslinked
-150
-100
-50
0
50
100
150
Temperature (°C)
b
1.0E+09
1.0E+08
1.0E+07
1.0E+06
Loss modulus E'' (Pa)
gelatin
gelatin-pectin
crosslinked
-150
-100
-50
0
50
100
150
Temperature (°C)

Figure 13

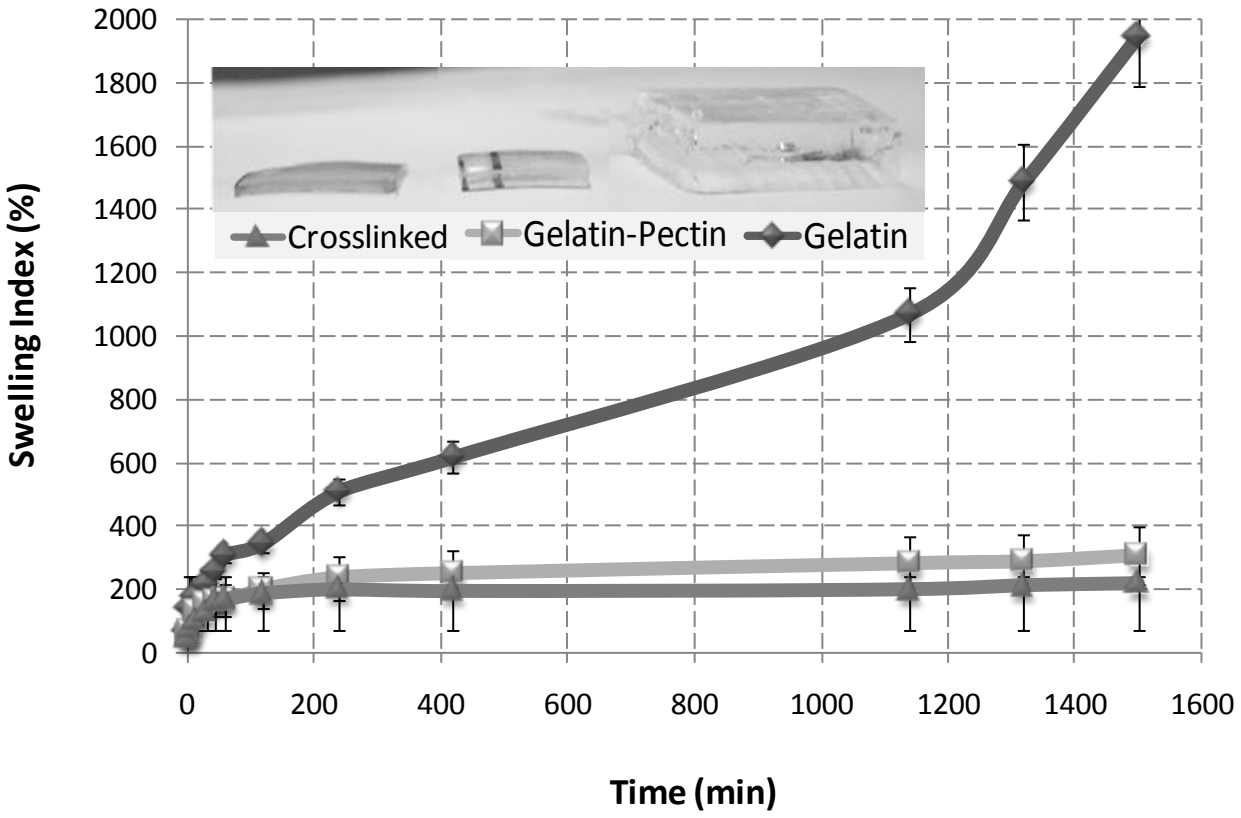
Swelling Index (%)
2000
1800
1600
1400
1200
1000
800
600
400
200
0
0
200
400
600
800
1000
1200
1400
1600
Crosslinked
Gelatin-Pectin
Gelatin
Time (min)

Table 1

Table 1. Mechanical properties of the three different types of composite films

Formulation	Parameter		
	Elastic Modulus (MPa)	Tensile strength (MPa)	Elongation (%)
Gelatin	0.5 ± 0.12^{a}	8.22 ± 0.92^{d}	115.33 ± 7.79^{g}
Gelatin-Pectin	0.28 ± 0.07^{b}	11.09 ± 1.51^{e}	151.57 ± 10.24^{h}
Crosslinked	0.35 ± 0.04^{c}	21.59 ± 3.74^{f}	159.1 ± 16.26^{h}

Results are expressed as a mean ± standard deviation.
Different letters denote statistically significant differences ($p < 0.05$) between formulations.